Astron. Astrophys. 321, 803–810 (1997)

ASTRONOMY
AND
ASTROPHYSICS

Spectrophotometry of flares and short time scale variations in weak line, and classical T Tauri stars in Chamaeleon

Eike W. Guenther[1,2] **and James P. Emerson**[2]

[1] Thüringer Landessternwarte Tautenburg, Karl-Schwarzschild-Observatorium, D-07778 Tautenburg, Germany
[2] Department of Physics, Queen Mary & Westfield College, Mile End Road, London E1 4NS, UK

Received 3 September 1996 / Accepted 21 October 1996

Abstract. Results are presented from a monitoring program looking for variations of the equivalent width and flux of Hα, and of the continuum flux, in 18 classical and 18 weak line T Tauri stars, and one Herbig Ae/Be star, on time scales down to 5 minutes. The stars were observed simultaiously for 14 hours using the multiobject-spectrograph FLAIR on the UK Schmidt Telescope. The campaign turned up two events in weak line T Tauri stars. Both events show the characteristics of flares: The increase of the Hα emission is faster than the decline, and the increase of the emission is much larger in Hα than in the continuum. The total energies radiated in Hα are $2.0 \pm 0.7 \times 10^{33}$ erg and $\geq 6 \pm 2 \times 10^{32}$ erg, or roughly 200 to 700 times larger than the largest flares on the Sun. The spectrum of one of these events shows a component of Hα which is blue-shifted by about 600 km^{-1}. We interpret this component as an indication of mass loss, and estimate, if the event is a typical one, that the mass loss rate due to flares would be about 10^{-13} M$_\odot$ yr^{-1} for a weak line T Tauri star. We derive lower limits to the magnetic flux density of between 10 and 200 G. Although a number of events have been observed in the classical T Tauri stars as well, none of these has shown the strong increase within minutes and decrease in an hour characteristic of a flare. We interpret this result as being due to either an optical thickness effect in Hα, or to the absence of optical flares in classical T Tauri stars, or simply due to failing to catch any flares in classical T Tauri stars.

Key words: stars: pre-main-sequence – stars: flares – stars: magnetic fields – stars: mass loss – stars: emission-line

1. Introduction

Classical T Tauri stars (cTTSs) are young, low-mass pre-main-sequence stars, with a circumstellar accretion disk. For a long time it has been a mystery how these stars can keep their low rotation rates while accreting matter from the disk. Currently, the most popular model is that a magnetic field with a strength of about 1000 G couples star and disk, such that angular momentum is transported outward, while matter is flowing inwards. Since direct measurements of the fields are still rather sparse, evidence that strong magnetic fields are involved comes only from indirect arguments (see review by Edwards 1995).

One very important argument for the presence of magnetic fields is that the X-ray emission shows occasional rapid increases (Feigelson & DeCampli 1981, Walter & Kuhi 1984, Montmerle et al. 1993, Preibisch et al. 1993). The events were canonically interpreted as flares, like flares on the Sun (or in flare stars) but of enormous energy output. The X-ray spectra indeed indicate high temperatures and rapid increase and slow decrease which are characteristic of flares (Preibisch et al. 1993). Thus, the X-ray events are very likely to be flares. Using the observed temperatures and decay times of a giant X-ray flare on the cTTS LkHα92, Preibisch et al. (1993) were able to derive a minimum value of the magnetic flux density of 210 G, and volumes of 2×10^{33} cm^3 which implies that very strong magnetic fields are present.

However, for this analysis it has to be assumed that the basic flare structure and mechanisms are the same as on the Sun. From solar observations it is known that flares not only emit X-rays but also all kinds of radiation from radio waves up to gamma rays. Although the optical emission is a secondary effect, it is a necessary ingredient of a flare, and if the interpretation of the X-ray data is correct, optical flaring has to be observable (Somov 1992). Since the optical emission comes from the foot-points of the flaring loops, and the X-ray emission from the top, the detection or non detection of optical flares would tell us how closely the flares on cTTSs resemble the flares on the Sun, and thus if the use of scaled-up solar models is justified at all.

Since rapid increases of the optical brightness and spectral line variations on time scales of less than an hour have been observed on cTTSs (for example Bastian & Mundt 1979), the picture seems, at first sight, to be rather consistent. For example, Kuan (1976) and Worden et al. (1981) observed the broad-band photometric variations of cTTSs with a time resolution of a few seconds and found a $\sim$ frequency^{-2} distribution in the

Send offprint requests to: E. W. Guenther

power spectrum, similar to the flare-activity of UV Ceti stars. However, Gahm (1990) concluded from a statistical analysis of broad-band photometry that the events seen in cTTS are much redder than flares seen in flare stars and on the Sun, and do not show the characteristic light curves. This conclusion is further supported by a simultaneous spectroscopic and photometric monitoring of two cTTSs (for 50.8 hours) and three weak line T Tauri stars (wTTSs) (for 57.8 hours) by Gahm et al. (1995). Although these authors found three flares in wTTS with the characteristic rapid increase in Balmer-line and Balmer-continuum emission, no flare was seen in cTTS. In cTTS, all changes on time-scales of hours were slow and smooth, and probably due to variable extinction or variations of the veiling continuum. However, X-ray flares on cTTS are very rare, and the fraction of the time with significant short-term X-ray variability is 0.05 (Gahm 1990). Given the limited statistics of the data which are presently available, it can thus not be excluded that X-ray flares, unexpectedly, have no optical counterparts. The best possibility of resolving this possible discrepancy would be to monitor cTTSs simultaneously in X-rays and in the optical regime. The problem with this method again is the rarity of the events, and the most likely result of such a campaign thus would be that no flares are observed in the X-ray or in the optical regime.

Another approach, adopted here, is to obtain spectra of these events. Since wTTSs are similar to cTTSs, except that the former lack accretion and a massive disk, any event seen in wTTS has to be a flare rather than an accretion event. By observing wTTSs spectroscopically we will learn how a flare on a T Tauri star should look, which can then be compared with observations of cTTSs, and magnetically active stars, like dMe stars. Spectra are more suitable to distinguish flares from other events, because flares are characterised by a sudden increase and slow decrease of Balmer-line (and continuum) emission. Additionally, the line profiles occasionally show a pronounced blue-asymmetry. In this paper, we present the results from a simultaneous monitoring campaign of 18 cTTS, 18 wTTS and a Herbig Ae/Be star (HAeBe star) using the multi-object spectrograph FLAIR II on the UK Schmidt telescope. The FLAIR II has the advantage that spectra of many stars can be taken simultaneously, thus increasing the probability of observing rare events.

2. Observations and data-reduction

2.1. Setup

For our observations, we used the multi-object spectrograph FLAIR II (fiber-linked array-image reformatter) on the UK Schmidt telescope (see Parker & Watson 1995). We placed 18 fibers on cTTSs, 18 on wTTSs, and one on a HAeBe star. The T Tauri stars were selected from the HBC (Herbig & Bell 1988), and from optically identified ROSAT sources (Alcalá 1994) in the Chamaeleon T1 association. Additionally, six fibers were placed onto blank fields for sky subtraction, and two fibers onto non-variable stars (CPD-74 8094, CPD-75 723) of known brightness serving as flux standards. With this set-up we took 4 spectra of each object during the first observing night (J.D 244 9744), 54 spectra on the second (J.D 244 9746), 31 spectra on the third (J.D. 244 9747), and 55 on the last night (J.D. 244 9748). In total, 5328 spectra of T Tauri stars and of the HAeBe star were taken. The cTTSs were thus monitored for 253 hours, the wTTSs for 253 hours (18×14 hours), and the HAeBe star for 14 hours. We observed the spectral region around Hα (5350-6870 Å), typical integration times were 200 to 300s which gave a typical time resolution between 270s and 370s and spectral dispersion of 2.6 Å per pixel. The spectra were wavelength calibrated by using a Hg-Cd arc. Dome-flats were used for flat-fielding. Standard IRAF routines (dohydra) were used for flat-fielding, sky-subtraction, extraction of the spectra, and for wavelength calibration.

2.2. Flux calibration

The simultaneous observations of CPD-74 8094 and CPD-75 723 allowed us to obtain a rough flux-calibration. The brightness of the flux-standards in the 5350-6870 Å region were derived by using the spectral types and the photometric data from the SIMBAD catalogue, and the spectral energy distribution of stars with similar spectral-types from Jacoby et al. (1984). The transmission of the individual fibers were measured by using the dome-flats. The main problem in flux calibration is the atmospheric refraction, because we had to observe the cluster at zenith distances of up to 60 degrees. At such large zenith distances, the stars are not any longer centred in the middle of the fibers (diameter 6.7 arcsec as projected on the sky), and hence some of the flux is being lost. The effect of change in the atmospheric refraction could partly be compensated by rotating the plate-holder every half an hour. From the measurements of the fluxes of the standard stars, we derive an error of 24.2% for the absolute-photometry, and 8.8% for the relative-photometry. The photometric accuracy will be somewhat better for the 25 stars that are closer to the centre than the flux-standards, and worse for the 11 stars that are further away from the centre of the field. The errors of the flux measurement in the continuum and Hα are computed from the photon statistics, and the variance of the standard stars Since the measurement of the equivalent width is not spoiled by the problems of the flux calibration, it is better to search for flares by monitoring the changes in the equivalent width, rather than the line-fluxes. The continuum and line flux measurements were then used for those events that were detected by changes of the equivalent width. Compared to the work by Gahm et al. (1995) our photometric accuracy is much worse. However, the time resolution is typically a factor 15 better, and FLAIR II allows us to monitor the stars for 518 hours compared to 50.8 hours.

3. Weak line T Tauri stars

As was shown in Guenther & Hessman (1996), variations of the equivalent width and the line-fluxes are tightly correlated. We will use the measurements of the equivalent widths to detect variations because these measurements are not effected by any problems of the flux-calibration. Table 1 lists the general

properties and the results of the measurement of the equivalent widths for all 37 pre-main sequence stars observed. The stars are ordered according to the measured equivalent width of Hα (column 5), the spectral type is taken from the literature (Herbig & Bell, 1988; Alcalá 1994) Column 7 contains the night-to-night variations of the equivalent width, column 8 gives the average variations of the equivalent width during the night (typically 4 hours), and column 9 contains the uncertainties of the measurements.

We found that the variability of the wTTS is normally very small. Significant night to night variations ($> 3\sigma$) were only detected in J1111.7-7620 (the night-to-night variation in J1039.5-7538 is 2.1 σ only). Similarly, the variations of the equivalent width within a night were usually also very small, as the average variations of the equivalent width during the night were smaller than 2σ in all wTTSs, except for J1014.2-7636 which was 2.6σ. With few exceptions, the wTTSs are thus very constant and do not show variability on timescales up to 120 hours. However, by inspecting the time series data for each wTTS and night individually we detected three clear events in which the equivalent width changed in a relatively short time which we will discuss in more detail below.

3.1. Results for the individual wTTSs

J1149.8-7850

On the second night (J.D. 244 9746) we observed that the Hα equivalent width increased from 3.27 ± 0.82 Å to 6.70 ± 0.82Å in 24 minutes. In the same time, the flux of Hα increased from $5.1 \pm 2.2 \times 10^{-14}$ erg s^{-1} cm^{-2} to $13.1 \pm 3.6 \times 10^{-14}$ erg s^{-1} cm^{-2}. The rapid increase was followed by a slow decay. In about 160 minutes the equivalent width declined to 4.3 ± 1.8 Å , and the line-flux decreased to $1.16 \pm 0.31 \times 10^{-14}$ erg s^{-1} cm^{-2}. The total energy released in this event in Hα is $\sim 6 \times 10^{-10}$ erg cm^{-2}. Fig. 1 shows the light-curve of the event, and Fig. 2 some of the spectra. We measured a continuum-flux of $1.57 \pm 0.56 \times 10^{-14}$ erg s^{-1} cm^{-2} Å^{-1} before the flare, $1.96 \pm 0.48 \times 10^{-14}$ erg s^{-1} cm^{-2}Å^{-1} during the flare, and $1.16 \pm 0.31 \times 10^{-14}$ erg s^{-1} cm^{-2} Å^{-1} after the flare. The errors quoted above are the errors of the absolute photometry. However, as explained in Sect. 2.2, the errors of the relative photometry much smaller. In the case of J1149.8-7850 they are 11.2% The continuum flux-increase of 24.8% and flux-decrease of 69.0% in J1149.8-7850 are thus 2.2σ and 6.2σ events, and are thus is likely to be real.

It might be that the increase in the continuum did occur somewhat earlier than the increase in Hα, so that the pre-event values were already enhanced. Spectra taken during the high state show a very pronounced blue-asymmetry in Hα. The line-wings (Fig. 2b) extend up to at least -1000 km/s, in the blue wing. The red wing remains constant during the event. This blue asymmetry will be discussed in the next section. The rapid increase, the slow decrease and the pronounced blue asymmetry of the Hα line-profile are very typical of flares, like flares on the Sun or on dMe stars. After subtracting the pre-flare spectrum from the flare spectrum the He I 5876 line with an equivalent width of 1.34 ± 0.31 Å became visible. The detection of the He I 5876 line implies that the temperature of the emitting region is at least 10,000 K and more likely 20,000 to 30,000 K.

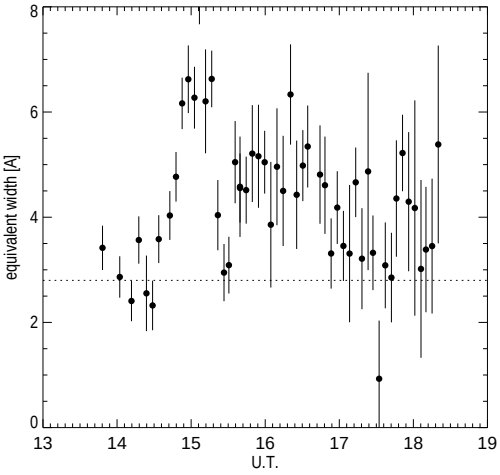

Fig. 1. Equivalent width of Hα of the weak line T Tauri star J1149.8-7850 on J.D. 244 9746. The equivalent width changes within 24 minutes from about 3.3 Å to 6.7 Å and then decreases slowly in about 160 minutes.

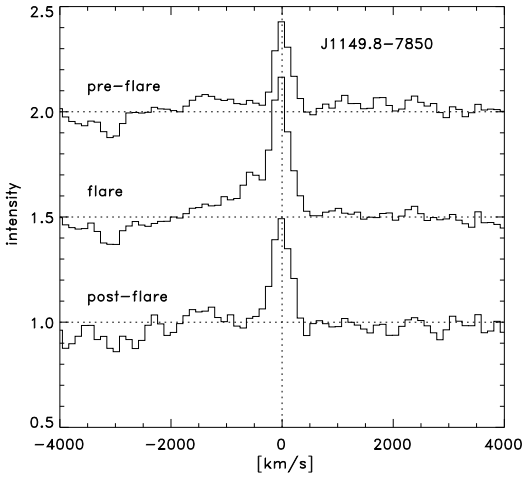

Fig. 2. Pre-flare, flare, and post-flare spectra from J1149.8-7850 near Hα. The pre-flare spectrum is an average of 6 spectra taken U.T. 13.80 to 14.56 (J.D. 244 9746.075-J.D. 244 9746.107). The flare spectrum is an average of 6 spectra taken U.T. 14.71 to 15.11 (J.D. 244 9746.113-J.D. 244 9746.130). The post-flare spectrum is an average of 6 spectra taken between U.T. 16.08 to 16.51 (J.D 244 9746.170-J.D 244 9746.188). The spectra are normalised to the local continuum, the continuum-flux increase of 25% is thus not shown. The line-profile of Hα shows a pronounced blue-asymmetry during the flare.

J1106.3-7721

J1106.3-7721 shows a slow and steady decay on the last observing night. In the 348 minutes of our monitoring, the

Table 1. Properties of stars and results

type	name of the star	X-ray[1] [cts/ks]	spectral type	EW Hα[2] [Å]	Flux Hα [10^{-14}erg s^{-1}cm^{-2}]	n-n[3] σ [Å]	w-n[4] σ [Å]	uncertainty[5] [Å]
cTTS[8]	HM 27		K7[8]	136.3 ± 14.9	20.5 ± 1.6	26.54	22.53	± 17.49
cTTS[8]	VZ Cha	13.5 ± 1.5[6]	K6[8]	75.4 ± 6.4	97.8 ± 11.3	7.48	2.15	± 1.18
cTTS[8]	VW Cha	5.5 ± 1.0[6]	K2[8]	72.5 ± 7.2	16.2 ± 28.0	8.24	2.19	± 0.79
cTTS[8]	VV Cha	6.2 ± 1.7[6]	M1.5[8]	69.3 ± 8.4	17.6 ± 4.0	9.83	5.54	± 4.68
cTTS[8]	HM 32	33.5 ± 4.0[6]	M0.5[8]	45.7 ± 7.7	23.3 ± 4.9	13.47	2.32	± 1.71
cTTS[8]	CV Cha		G8V[8]	45.5 ± 3.0	242.8 ± 47.0	5.60	0.77	± 0.35
cTTS[8]	WX Cha	3.1 ± 0.7[6]	K7,M0[8]	42.3 ± 25.1	18.4 ± 9.9	26.89	2.84	± 1.92
cTTS[8]	WY Cha	17.7 ± 1.7[6]	K7,M0[8]	41.3 ± 3.5	29.3 ± 3.5	3.11	2.18	± 1.28
cTTS[8]	Sz 6		K2[8]	38.1 ± 1.9	252.4 ± 32.8	2.45	0.73	± 0.27
cTTS[8]	SX Cha		M0.5[8]	33.2 ± 7.2	11.0 ± 3.00	7.36	3.20	± 2.03
cTTS[8]	WW Cha	7.5 ± 1.1[6]	K5[8]	30.8 ± 4.0	26.9 ± 5.6	3.67	2.16	± 0.92
cTTS[8]	CS Cha	40.1 ± 2.8[6]	K5[8]	28.6 ± 6.3	118.8 ± 27.4	6.61	1.26	± 0.31
cTTS[8]	TW Cha	13.6 ± 1.8[6]	M0[8]	28.3 ± 5.7	21.6 ± 8.0	7.27	1.32	± 1.14
HAeBe[8]	CU Cha		A0[8]	20.1 ± 12.4	$1057.0 \pm 642.$	15.15	0.54	± 0.07
cTTS[8]	SY Cha	8.7 ± 1.7[6]	M0[8]	17.5 ± 1.9	19.0 ± 8.3	3.85	0.99	± 0.81
cTTS[8]	LHa332-17		G2[8]	15.1 ± 0.8	137.1 ± 26.1	0.92	0.23	± 0.16
cTTS[8]	Sz 18		M2,3[8]	11.8 ± 11.3	2.4 ± 3.6	14.49	2.38	± 1.86
wTTS[7]	J1150.9-7411	110 ± 41[7]	M4[7]	6.7 ± 3.7	2.0 ± 1.0	1.55	2.16	± 1.61
wTTS[7]	J1014.2-7636	62 ± 22[7]	M2[8]	5.6 ± 1.8	1.6 ± 0.7	1.48	5.04	± 1.88
cTTS[8]	Sz 41			4.1 ± 16.2	0.088 ± 0.59	2.60	15.21	± 12.1
cTTS[8]	UV Cha			4.0 ± 15.7	0.47 ± 0.55	3.36	11.95	± 5.48
wTTS[7]	J1111.7-7620	83 ± 27[7]	K3[7]	2.9 ± 1.7	6.2 ± 3.6	1.56	0.33	± 0.33
wTTS[7]	J1202.8-7718	87 ± 16[7]	K7[7]	2.7 ± 1.2	0.75 ± 0.73	0.36	1.95	± 1.43
wTTS[7]	J1204.6-7731	97 ± 17[7]	M3[7]	2.7 ± 1.4	1.4 ± 0.7	0.64	1.59	± 1.10
wTTS[7]	J1149.8-7850	125 ± 38[7]	M0[7]	2.1 ± 1.4	1.3 ± 1.1	0.70	1.18	± 0.96
wTTS[7]	J1158.5-7754	445 ± 38[7]	M2[8]	1.2 ± 1.8	0.42 ± 0.47	0.44	1.40	± 1.75
wTTS[7]	J1108.8-7519	60 ± 23[7]	M2[7]	0.1 ± 0.9	0.058 ± 0.68	0.28	0.78	± 0.67
wTTS[7]	J1044.6-7849	58 ± 16[7]	M2[7]	0.1 ± 1.2	0.053 ± 0.514	0.39	1.23	± 1.23
wTTS[8]	SZ Cha	11.9 ± 1.8[6]	K0[8]	-0.2 ± 0.5	-0.8 ± 1.9	0.44	0.21	± 0.24
wTTS[7]	J1048.9-7655	54 ± 22[7]	K6[7]	-0.8 ± 1.3	-1.0 ± 1.1	0.63	0.89	± 0.54
wTTS[7]	J1150.4-7704	108 ± 24[7]	K2[7]	-0.8 ± 0.3	-1.9 ± 0.7	0.08	0.25	± 0.32
wTTS[7]	J1120.3-7828	339 ± 32[7]		-1.1 ± 0.3	-6.7 ± 2.4	0.20	0.16	± 0.19
wTTS[7]	J1108.2-7728	46 ± 21[7]	K6[7]	-1.2 ± 0.6	-1.7 ± 0.8	0.22	0.58	± 0.46
wTTS[7]	J1159.7-7601	125 ± 26[7]	K2[7]	-1.5 ± 1.3	-2.0 ± 1.8	0.59	1.02	± 0.60
wTTS[7]	J1129.2-7546			-1.9 ± 0.6	-2.8 ± 0.9	0.004	0.51	± 0.44
wTTS[7]	J1106.3-7721	99 ± 23[7]		-2.1 ± 0.3	-14.3 ± 3.1	0.12	0.20	± 0.15
wTTS[7]	J1039.5-7538	312 ± 56[7]		-3.9 ± 0.2	-74.4 ± 11.6	0.19	0.10	± 0.09

1) counts per kilo-second by ROSAT
2) statistical error of the equivalent width (EW) as derived from the variance of the measurements
3) variations of the equivalent width from night to night
4) variations of the equivalent width within one night
5) error of the measurement of the equivalent width as computed from the readout noise and the photon statistics
6) from Feigelson et al. 1993
7) from Alcalá 1994
8) from Herbig & Bell 1988

flux in Hα decreased from $10 \pm 3 \times 10^{-14}$ erg s^{-1} cm^{-2} to $2.3 \pm 1.4 \times 10^{-14}$ erg s^{-1} cm^{-2}. Correspondingly, the equivalent width decreased from 1.4 ± 0.3 to 0.5 ± 0.3Å. There might be a change in the continuum emission, as the continuum emission decreased from $7.2 \pm 1.8 \times 10^{-14}$ erg s^{-1} cm^{-2} Å^{-1} to $4.7 \pm 1.2 \times 10^{-14}$ erg s^{-1} cm^{-2} Å^{-1}. This event could have been the decay phase of a flare the rise of which we did not observe. As we cannot however be sure that the rise was fast, as for a flare, we do not count it as a flare event here.

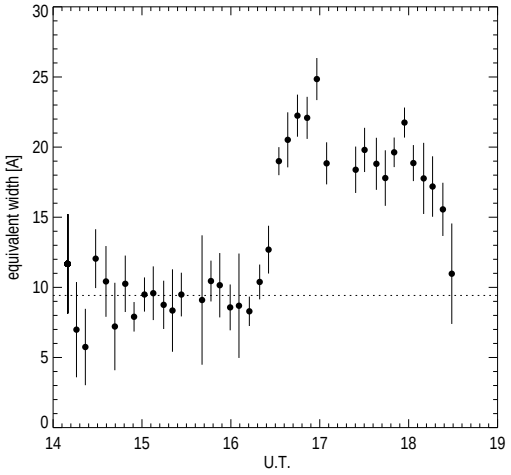

Fig. 3. Equivalent width of Hα of the weak line T Tauri star J1150.9-7411. The equivalent width increases within 30 minutes from about 9.2 Å to 23.1 Å and then decreases slowly.

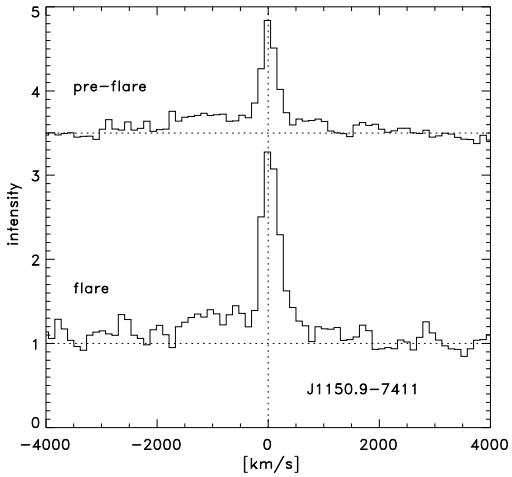

Fig. 4. Pre-flare, flare, and post-flare spectra from J1150.9-7411 near Hα. The pre-flare spectrum is an average of 6 spectra taken U.T. 15.78 to 16.42 (J.D. 244 9748.153-J.D. 244 9748.184). The flare spectrum is an average of 6 spectra taken U.T. 16.86 to 17.41 (J.D. 244 9748.202-J.D. 244 9748.225). The spectra are normalised to the local continuum. The line-profile of Hα is basically symmetric before and during the flare. However, the flare-spectrum does not include data from the first half an hour after the beginning of the flare.

J1150.9-7411

J1150.9-7411 shows a rather similar event to J1149.8-7850. The Hα line increased dramatically on the last night (J.D. 244 9748) from 9.2 ± 2.0 Å to 23.1 ± 1.55 Å in about 30 minutes (see Fig 3.). We followed the event for the next two hours, during which the flux slowly declined. Due to sunrise we were not able to follow the event until the flux reached the normal level again. From the decline rate we estimate that it might have taken another hour or two until Hα would have reached its normal values again. The line-flux increased from $2.2 \pm 0.8 \times 10^{-14}$ erg s^{-1} cm^{-2} to $7.1 \pm 2.8 \times 10^{-14}$ erg s^{-1} cm^{-2}. As in J1149.8-7850, we derived an increase of the continuum flux of 29% which is less than the error of the absolute photometry. In the case of J1150.9-7411, the error of the relative photometry is about 18% because the star is much fainter. The continuum flux-increase is thus 1.6 σ only, and might not be real.

Since our observations do not completely cover the event, we can only give a lower limit of the energy released. The lower limit of the energy release in $H\alpha$ is: $\geq 6 \pm 2 \times 10^{33}$ erg. Blue and red wings remain constant during the event. We derived an upper limit of 1.0Å for the HeI5876 line. The non-detection of the He I 5876 line implies that the temperature of the emitting region is most likely cooler than 30,000 K.

3.2. Discussion on the short time-scale variations of the wTTSs

The rapid increase, the slow decrease, and the line-profile of the events observed in J1149.8-7850 and J1150.9-7411 are very typical of flares. Using a distance of 140pc (Alcalá, 1994) for both stars, we derive the total energy released in Hα in J1149.8-7850 as $\sim 2 \cdot 10^{33}$erg, and $\geq 6 \cdot 10^{32}$erg in J1150.9-7411. Table 2. summarises the results of the observations of the two flares.

The largest flares on the Sun release about 5×10^{32} erg of which 3×10^{30} erg are released in Hα (Somov 1992). The flares in observed wTTS are thus about 200 to 700 times larger than the largest flares on the Sun. In the case of J1149.8-7850, we detect an increase of the continuum flux of about 24.8% or $9.1 \pm 4.1 \times 10^{27}$ erg s^{-1} Å^{-1}. For blackbody temperatures of 10,000 to 20,000 K this would correspond to U-band fluxes of $1.2 - 2.5 \times 10^{35}$ erg. These flares are thus well within the range of what was observed by Gahm (1990), who measured total energies in the U band in the range 2×10^{34} to 2×10^{36} erg on wTTS. The flares in J1149.8-7850 and J1150.9-7411 thus are about an order of magnitude larger than flares in UV Ceti stars (compare it, for example with Houdebine et al. 1990) but seem to be fairly typical for wTTS. From the observation of two flares in 253 hours of monitoring, we derive an observed flare-frequency of 70 ± 50 yr^{-1} (or a true flare-frequency of twice this when we note that flares on the far side of the star will be hidden from view) which is roughly the same as the observed frequency when the flux increases in the ultraviolet by more than 20% within 3 hours of 90 yr^{-1}, or as the observed frequency when a star shows significant short-term X-ray variability of 150 yr^{-1} (Gahm 1990). Significant X-ray variability, flux increase in the ultraviolet, and Hα flares are thus likely to be different manifestations of the same process.

An interesting feature of the spectrum of J1149.8-7850 is the blue asymmetry of the line profile during the flare (Fig. 2). The line-profile of Hα consists of two components: one component at the stellar rest velocity, the other one at about -600 km s^{-1}. The blue-shifted component in J1149.8-7850 is a clear sign of mass loss, because the line-of sight velocity is higher than the typical escape velocity of a wTTS (440 km/s for $R_* = 2R_\odot$ and $M_* = 1M_\odot$), and thus seems to be a scaled up version of the coronal mass ejections that are familiar from the Sun. The flux of the blue-shifted component is 33.2 ± 4.2% of the

Table 2. Summary of the properties of the two flares in wTTS

	J1149.8-7850	J1150.9-7411
J.D. of the peak of the flare	244 9746.12	244 978.21
rise time [min.]	24	30
decay time [min.]	160	> 100
equivalent width of Hα before the flare [Å]	3.27 ± 0.82	9.22 ± 2.02
equivalent width of Hα during the flare [Å]	6.70 ± 0.82	23.06 ± 1.55
equivalent width of Hα after the flare [Å]	3.68 ± 1.15	
flux of Hα before the flare [10^{-14}erg s^{-1} cm^{-2}]	5.1 ± 2.2	2.2 ± 0.8
flux of Hα during the flare [10^{-14}erg s^{-1} cm^{-2}]	13.1 ± 3.6	7.1 ± 2.8
flux of Hα after the flare [10^{-14}erg s^{-1} cm^{-2}]	4.3 ± 1.8	
continuum intensity before the flare [10^{-14}erg s^{-1}cm^{-2}Å^{-1}]	1.57 ± 0.56	0.237 ± 0.069
continuum intensity during the flare [10^{-14}erg s^{-1}cm^{-2}Å^{-1}]	1.96 ± 0.48	0.31 ± 0.12
continuum intensity after the flare [10^{-14}erg s^{-1}cm^{-2}Å^{-1}]	1.16 ± 0.31	
observed flux in Hα [10^{-10}erg cm^{-2}]	$\sim 6. \pm 2.$	$> 3. \pm 1.$
observed flux in the continuum [10^{-11}erg cm^{-2} Å^{-1}]	$\sim 4. \pm 1.$	-
total energy released in Hα [10^{33}erg]	$\sim 2.0 \pm 0.7$	$> 0.6 \pm 0.2$
energy released in the continuum [10^{31}erg Å^{-1}]	$\sim 9. \pm 3.$	-

flux of the main-component, or 2.8×10^{-14} erg s^{-1} cm^{-2}. Such line profiles have occasionally been observed in flares of dMe stars. For example, Gunn et al. (1994) observed a blue-shifted component with velocities of 400-600 km/s during a flare in the dMe star AT Mic in Hδ, Ca II H, Ca II K, and H8. Another high velocity mass ejection in the M-dwarf AD Leo was observed by Houdebine et al. (1990), in this event velocities of up to 5830 km/s were observed. In terms of the flux, the flare which we observed in J1149.8-7850 is one to three orders of magnitude larger than what is typically observed in the dMe stars. For example, if AD Leo were at a distance of 140pc, the peak flux of the flare in Hα would have been 2.3×10^{-15} erg s^{-1} cm^{-2} compared to 1.3×10^{-13} erg s^{-1} cm^{-2} in J1149.8-7850, and the total energy released in AD Leo in Hα would have been 4.3×10^{-13} erg cm^{-2} compared to 6×10^{-10} erg cm^{-2} in J1149.8-7850.

It is possible to get a very rough estimate for the mass loss rate from our observations. Houdebine et al. (1990) compute the mass loss for the event in AD Leo from the flux of the Hγ line using a density of emitted material of 10^{10} cm^{-3}, an opacity damping factor (O.D) for Hγ between two and five (20 to 50 % of the Hγ flux effectively escapes from the plasma), and temperatures of 20,000 K. The flux of the blue-shifted component of the flare in J1149.8-7850 in Hγ can be estimated from the observed Balmer decrement for solar and stellar flares of Hγ = Hα/3 (Butler et al. 1988). Since we detected the He I 5876 line, we estimate that the temperature of the emitting material in J1149.8-7850 is in the region 20,000 to 30,000 K. Table. 3 gives the *lower* limits for mass of the ejected material, kinetic energy and the emitting volume for the flare in J1149.8-7850 using a density of 10^{10} cm^{-3} for different temperatures and opacity damping factors. Table 3 also gives the total mass loss rate due to flares which can be calculated from these values if we assume that the event in J1149.8-7850 is rather typical for flares of wTTSs and that there are about 200 such flares per year ($\sim$ 90yr^{-1} doubled to account for flares on the far side of the stars). With a value for the temperature of 20,000 K we derive mass loss rates of the order of $\sim 10^{-13}$ M$_\odot$ yr^{-1}. For higher temperatures and lower densities, the mass loss rate would become substantially higher.

We did not measure the increase in continuum flux in the whole optical spectrum but from our measurements close to Hα and by assuming temperatures of 10,000 to 30,000 K for the flare in J1149.8-7850, we estimate that the flux released in the optical regime is $\sim 10^{34}$ erg. The total energy released in the flare in J1149.8-7850, including the kinetic energy of the emitted material will thus be of the order of 10^{34} to 10^{35} erg. Using this range of energies and the volumes of the emitting material from Table 3, we derive a lower limit of the magnetic flux density between 10 and 200 G. These values are very close to the 210 G deduced by Preibisch et al. (1993) for the flare in LkHα 92, and of the same order of magnitude as in solar flares (Haisch et al. 1991). The difference between flares on the Sun, and the flare on J1149.8-7850 thus is emitting volume and hence the total energy released and, not the magnetic flux density.

4. Classical T Tauri stars and the Herbig Ae/Be star

4.1. Results for the individual cTTSs

Although a number of cTTSs did show some variations during the night, the only star where the average variations during the typical 4 hours of observations per night is larger than 3σ is CS Chamaeleon (see Table 2). However, by inspecting the time series data for each cTTS and night individually we detected some variations in Sz 6, VZ Cha & CU Cha (the HAeBe star HD97048), which did not show an excess in the averages in Table 1. In the following we will discuss these variations, the interpretation will be given in Sect. 4.2.

Table 3. Lower limits for the the mass, kinetic energy and volume of the ejected material in J1149.8-7850. The mass loss rate assumes 200 such flares per year.

T_e [K]	opacity damping factor [Hγ]	mass of the ejected material [g]	kinetic energy [erg]	mass loss rate $M_\odot yr^{-1}$	emitting volume [cm^{-3}]
20000	2	$1.4 \cdot 10^{18}$	$2.5 \cdot 10^{33}$	$1.4 \cdot 10^{-13}$	$6.2 \cdot 10^{31}$
20000	5	$3.4 \cdot 10^{18}$	$6.2 \cdot 10^{33}$	$3.4 \cdot 10^{-13}$	$1.6 \cdot 10^{32}$
30000	2	$3.1 \cdot 10^{19}$	$5.6 \cdot 10^{34}$	$3.1 \cdot 10^{-12}$	$1.4 \cdot 10^{33}$
30000	5	$7.8 \cdot 10^{19}$	$1.4 \cdot 10^{35}$	$7.8 \cdot 10^{-12}$	$3.5 \cdot 10^{33}$

CS Chamaeleon

As shown in Table. 1, the variations CS Cha during the night are about 4.06σ. In the second night (J.D 244 9746), the equivalent width of Hα decreased from 38.7 ± 0.3Å to 34.4 ± 0.3 Å in 4.4 hours, corresponding to -0.96 ± 0.03 Å h^{-1}. The equivalent width on the next night (J.D. 244 9747) was found to be smaller and still decreasing. The equivalent width was 24.2 ± 0.4 Å exactly 24 hours later. The average gradient in the meantime must have been -0.43 ± 0.10 Å h^{-1}. The gradient in the third night was found to be -0.67 ± 0.15 Å h^{-1}. The equivalent width of Hα was 22.1 ± 0.4 Å. In the last observing night the gradient reversed and became 2.77 ± 0.10 Åh^{-1}.

Sz 6

The only variation seen in Sz 6 is a slow decline of the equivalent width in the last observing night (J.D. 244 9748). The equivalent width decreased from 39.8 ± 0.3 to 34.3 ± 0.3 Å in 5.8 hours. The gradient thus is 0.95 ± 0.07 Å h^{-1}

VZ Chamaeleon

Smooth and steady variations characterised the variations during the night of VZ Cha. On the second observing night (J.D. 244 9746), the equivalent width increased from 67.0 ± 0.7 Å to 70.2 ± 1.0 Å, and in the third night from 74.9 ± 1.6 Å to 80.6 ± 1.5 Å in 3.4 hours. The gradient in the second and third nights (J.D. 244 9747) thus were 0.70 ± 0.28 Å h^{-1}, and 1.65 ± 0.63 Å h^{-1}, respectively. The equivalent width was basically constant on the fourth night (J.D. 244 9748). We observed an increase of the equivalent width from 81.3 ± 0.9 Å to 84.1 ± 1.3 Å in 50 min and down to 80.3 ± 1.4 Å in 120 min. Since the flux in Hα in this night was $112.3 \pm 17.7 \cdot 10^{-14}$ erg s^{-1} cm^{-2}, the increase corresponds to $4.4 \pm 1.8 \cdot 10^{-14}$ erg s^{-1} cm^{-2} which is of the same order as the events in J1150.9-7411 and J1150.9-7411. However, this event is just two σ above the noise level, and thus probably not real as discussed further below.

The Herbig Ae/Be star CU Chamaeleon (HD 97048)

Except for the last observing night (J.D. 244 9748), the equivalent width of Hα remained constant during the night. In the last observing night, CU Chamaeleon showed a slow and steady decrease of the equivalent width from 27.28 ± 0.09 Å to 25.26 ± 0.15 Å in 5.8 hours. The gradient was thus 0.34 ± 0.15 Å h^{-1} only.

4.2. Discussion on the short time-scale variations of the cTTSs and the Herbig Ae/Be star

Although, as described in the previous sub-section, some variations in the cTTS were observed during the night, all these variations are slow and smooth increases or decreases of the equivalent width of Hα. We did not detect anything like the flare-like events seen in the wTTSs J1149.8-7850 and J1150.9-7411. The gradients of the short-time scale variations in cTTS are not substantially larger than the gradients of the night-to night variations, and are probably due to a change of the accretion rate.

Since the Hα equivalent width of the cTTS is much larger than the Hα equivalent width of the wTTS, one might think that any small increases due to flares in the cTTS might be hidden in the noise. We measured an increase of the flux of 8.0×10^{-14} erg s^{-1} cm^{-2} and 4.9×10^{-14} erg s^{-1} cm^{-2} in J1149.8-7850 and J1150.9-7411. An increase of 4×10^{-14} erg s^{-1} cm^{-2} during a flare would be larger than 4σ in HM 32, Sz 18, Sz 41, SX Cha, SY Cha, TW Cha, UV Cha, VW Cha, WW Cha, WX Cha, and WY Cha, between 3σ and 4σ in CS Cha, and VV Cha, between 2σ and 3σ in VZ Cha, CV Cha, Sz 6, and LHα332 an less than 2σ in CU Cha, and HM 27. VZ Chamaeleon thus falls into the category of stars where events like those observed in wTTS could not have been detected, and the $4.4 \pm 1.8 \times 10^{-14}$ erg s^{-1} cm^{-2} has to be regarded as non-significant. Thus, flares should in principle be detectable in roughly 2/3 of the cTTSs of our sample. The results of our observations thus somewhat deepen the mystery in that there are no, or at least very few, optical flares in cTTSs. However, these results are in good agreement with the results of Gahm (1990) and Gahm et al. (1995).

There are three possible explanations for the non-detection of flares in the cTTSs:

- Just by chance no flares occurred in a cTTSs, although their frequency is the same as in wTTSs (in which we saw two events). The probability for this is 0.25.
- It could be that the flares originate very close to the star. If much of the Hα emission originates at large distances, flares could not be observed if Hα is optically thick in cTTSs.

– There are no, or only very few, optical flares in cTTSs, because either the majority of cTTSs lack magnetic fields (the few flares seen in the X-rays might come from peculiar sources), or because the flares on cTTSs are really not solar-like, and do not give rise to an Hα emission line.

5. Conclusions and outlook

Our observing run with FLAIR II clearly demonstrated that flares on TTs can effectively be observed with this instrument. We actually observed two flares in weak line T Tauri stars. The properties of these flares closely resemble our expectations, which means that the flares on wTTSs seem to be scaled up versions of flares on dMe stars or the Sun. The results from this observing run thus are another piece of evidence that wTTS have strong magnetic fields.

Spectra of one of these events show a second component of Hα which is blueshifted by 600 km^{-1}. We interpret this feature as a clear sign of mass loss, similar to what has been observed in dMe stars. The fluxes of the lines are, however one to two orders of magnitude larger than those in a dMe star. We estimate that the mass loss rate due to flares could be as high as $10^{-13}\,M_{\odot}yr^{-1}$ for temperatures of 20,000 K. Like on the Sun, we can expect that a substantial fraction of the ejected material are high energy protons ($E_p \geq 20$MeV) and electrons ($E_e \geq 20$keV) which will affect any circumstellar material.

We estimated a lower limit of the magnetic flux density between 10 and 200 G. These values are thus in excellent agreement with the X-ray data from the flare in the cTTS LkHα 92 by Preibisch et al. (1993). The difference between flares on the Sun, and on wTTSs is thus basically the emitting volume, not the magnetic field strength, as similar values have been observed in solar flares (Haisch et al. 1991). As we have shown in Sect. 4, the emitting volumes of the flares in wTTSs are enormous, and could be as large as the star itself (see Table 3) implying that the total magnetic flux of the star has to be very large. This clearly indicates that at least some wTTSs must have a large magnetic field in order to produce such flares.

We did not find any flares in the classical T Tauri stars of our sample. This is probably due an optical thickness effect in Hα, or perhaps simply due to bad luck. Obviously, more observations should be carried out, especially in the higher Balmer lines which have a smaller optical depth than Hα. Although the observations of strong flares in cTTSs would clearly indicate that these stars have magnetic fields, the non-observation of flares would not necessarily indicate that cTTSs do not have magnetic fields, because flares can only occur if magnetic field lines are twisted. For example, if T Tauri stars have well ordered dipole fields, flares could not occur, even if the field strength is very large.

Acknowledgements. We thank the staff of the UK Schmidt Telescope of the Anglo Australian Observatory for all their help and assistance in relation to FLAIR and also the UKST Unit of the Royal Observatory Edinburgh. Eike Guenther acknowledges financial support from PPARC. We acknowledge the assistance of STARLINK hardware and software in analysing our data.

References

Alcalá, J.M., 1994, Phd. Thesis University of Heidelberg
Bastian U., Mundt R., 1979, A&A 78, 181
Butler, C.J., Rodonó, M., Foing, B.H., 1988, A&A 206, L1
Edwards, S., 1995 In: Lizano, S., Torrelles, J.M. (eds.) Proceedings of the Circumstellar Disks, Outflows, and Star Formation Conference, Cozumel, Mexico, to appear in Revista Mexicana de Astronomia y Astrofisica
Feigelson, E.D., Casanova, S., Montmerle T., Guibert, J., 1993, ApJ 416, 623
Feigelson, E.D., DeCampli, W., 1981, ApJ 243, L89
Gahm, G.F., 1990, In: Mirzoyan, L.V., Pettersen, Tsvestkov, M.K., (eds.) Flare Stars in Star Clusters, Associations and the Solar Vicinity, IAU Symposium 137, Kluwer p. 193
Gahm, G.F., Lodén, K., Gullbring, E., Hartstein, D., 1995, A&A 301, 89
Guenther, E., Hessman, F.V., 1996, A&A, submitted
Gunn, A.G., Doyle, J.G., Mathioudakis, M., Houdebine, E.R., Avgoloupis, S. 1994, A&A 285, 489
Haisch, B.M., Strong, K.T., Rodonó, M., 1991, ARA&A 29, 275
Herbig, G.H., Bell, R.K., 1988, Third Catalog of Emission-Line Stars of the Orion Population, Lick Observatory Bulletin No. 1111
Houdebine, E.R., Foing, B.H., Rodonó, M., 1990, A&A 238, 249
Jacoby, G.H., Hunter, D.A., Christian, C.A., ApJS 56, 257
Kuan, P., 1976, AJ 210, 129
Montmerle, T., Feigelson, E.D., Bouvier, J., André, P., 1993, In: Levy, E.H., Lunine, J.I. (eds.) Protostars and Planets III, The University of Arizona Press, p. 68
Parker, Q.A., Watson F.G., 1995, SPIE, 2476
Preibisch, Th., Zinnecker, H., Schmitt, J.H.M.M. 1993, A&A 279, L33
Somov, B.V., 1992 *Physical Processes in Solar Flares*, Kluwer Academic Publishers, Dordrecht
Walter, F.M., Kuhi, L.V., 1984, ApJ 284, 194
Worden, S.P., Schneeberger, T.J., Kuhn, J.R., Africano, J.L. 1981, ApJ 244, 520

This article was processed by the author using Springer-Verlag LaTeX A&A style file *L-AA* version 3.